Organic Electronics 58 (2018) 63–68

Contents lists available at ScienceDirect

Organic Electronics

journal homepage: www.elsevier.com/locate/orgel

Impact of interface types on spin transport in heterostructures of graphene/hexagonal boron-nitride nanoribbons

Mei Wang[a], Xiaoteng Li[a], Yuan Li[c], Xi Zuo[a], Dongmei Li[a], Bin Cui[a,**], De-Sheng Liu[a,b,*]

[a] School of Physics, State Key Laboratory of Crystal Materials, Shandong University, Jinan, 250100, China
[b] Department of Physics, Jining University, Qufu, 273155, China
[c] School of Information Science and Engineering, Shandong University, Jinan, 250100, China

ARTICLE INFO

Keywords:
Interface types
Graphene/*h*-BN heterostructures
Negative differential resistance
Spin filtering effect

ABSTRACT

Using density functional theory in combination with non-equilibrium Green's functions, we investigate the spin transport in two heterostructures of graphene and hexagonal boron-nitride (*h*-BN) nanoribbons with C-B and C-N interfaces, respectively. Significant spin-filtering effect (over 80%) is observed in both C-B and C-N devices with bias ranging from 0 V to 0.3 V. Interestingly, the spin polarizations are opposite in these two devices, and prominent negative differential resistance (NDR) for both spin-up and spin-down currents is observed only in the C-N device. These findings provide insight into how the spin-transport properties of graphene/*h*-BN nanoribbons can be impacted by different types of interfaces of the heterostructures.

Since the first discovery in 2004, graphene [1] has attracted wide attention in the field of nanoscale electronic devices due to its unique lattice structure and excellent electronic properties [2–5]. Different strategies were proposed to regulate the electronic structures of graphene, such as surface adsorption [6], cutting [7], chemical decoration [8–12], and introduction of defects and/or an external transverse electric field [13–15]., Many investigations were also focused on the applications of graphene in spintronic devices due to its exotic spin-polarized edge states [16–18].

Recently, the rapid development of two-dimensional (2D) materials, such as hexagonal boron nitride (*h*-BN) [19], silicene [20], and M_OS_2 [21], has attracted tremendous attention. While some 2D materials have lattice structures similar to that of graphene, their electronic and electrical properties were shown to be significantly different. For instance, the monolayer of *h*-BN, which also has a honeycomb lattice, has a wide bandgap (about 4.5 eV) [22] and charge carriers are hardly to transport in such wide-gap 2D material. Interestingly, however, the graphene/*h*-BN heterostructures, which were successfully fabricated by a thermal catalytic CVD method and heteroepitaxial growth [23,24], were demonstrated to have much improved properties. For instance, He et al. revealed theoretically that the band gap of graphene/*h*-BN heterojunction is tunable and an insulator-metal transition can be obtained by increasing the width of the graphene segment [25]. Vacancy-induced spin polarization in graphene/BN heterostructures was also reported [26,27]. Recently, it was shown experimentally that the edge types at the interface of graphene/*h*-BN heterostructures is controllable and the formation of zigzag-linking edges is more favorable than that of armchair-linking edges during the patching growth [28]. As such, rich magnetic and electronic properties can be observed in graphene/*h*-BN heterostructures with different structures of the interfaces [29–34]. While these studies demonstrated the importance of interfaces in the graphene/*h*-BN heterostructures, some fundamental issues, such as the underlying mechanism of how zigzag edges with C-B and C-N interfaces impact the electronic and spin-transport properties, still remain unclear and a more detailed investigation is needed.

In this Letter, we present a theoretical investigation on zigzag graphene/*h*-BN heterostructures with two different types of interfaces, i.e., C-B and C-N interfaces, respectively. The spin-transport properties of these two structures are studied by using density functional theory (DFT) combining with non-equilibrium Green's function (NEGF) method. Our results, as will be shown, reveal that distinct behaviors of spin-filtering effect (SFE) and spin-dependent negative differential resistance (NDR) can be obtained in these two devices as a result of the different interfacial properties.

The graphene/*h*-BN heterostructures employed in this work has been shown in Fig. 1, in which graphene nanoribbons with 3 zigzag chains and *h*-BN nanoribbons with 6 zigzag chains are considered. Fig. 1(a) and (b) display the device structures with two different types of interfaces, i.e., C-B interface (M1) and C-N interface (M2), respectively. Each model device can be divided into three regions, i.e., the left

* Corresponding author. School of Physics, State Key Laboratory of Crystal Materials, Shandong University, Jinan, 250100, China.
** Corresponding author. School of Physics, State Key Laboratory of Crystal Materials, Shandong University, Jinan, 250100, China.
E-mail addresses: cuibin@sdu.edu.cn (B. Cui), liuds@sdu.edu.cn (D.-S. Liu).

https://doi.org/10.1016/j.orgel.2018.04.006
Received 10 February 2018; Received in revised form 26 March 2018; Accepted 3 April 2018
Available online 04 April 2018
1566-1199/

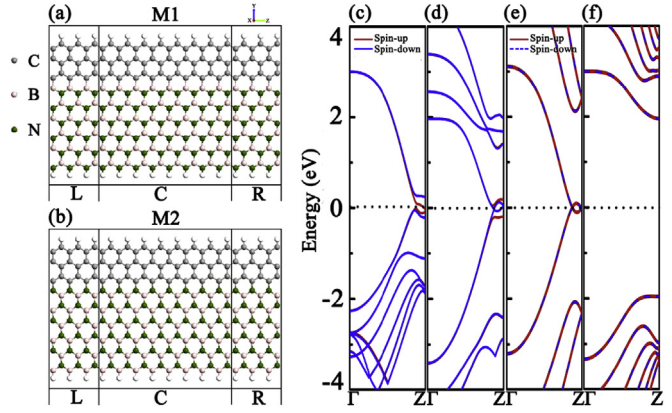

Fig. 1. (Color online) (a) and (b) Geometric structures of the C-B interface device (M1) and the C-N interface device (M2). L, C, and R denote the left electrode, the central scattering region, and the right electrode, respectively. The left/right electrode is semi-infinite in length. (c) and (d) Band structures calculated for the nanoribbons with C-B interface and C-N interface, respectively. (e) and (f) Band structures calculated for the pure graphene and *h*-BN, respectively. The dotted lines stand for the Fermi level, which is set to be zero. (For interpretation of the references to color in this figure legend, the reader is referred to the Web version of this article.)

electrode, the central scattering region, and the right electrode. Each electrode consists of a supercell with three repeated graphene/*h*-BN unit cells along the transport direction (i.e., the Z axis) and is semi-infinite in length. The vacuum layers between two sheets along the X and Y directions (as defined in Fig. 1) are set as 15 Å to keep the device from any interaction with its mirror images.

Calculations of both geometric optimizations and spin-dependent transport were performed by using spin-polarized density functional theory (DFT) in combination with non-equilibrium Green's function (NEGF) as implemented in the ATK software package [35–37]. Single-ζ plus polarization (SZP) basis set for the valence electrons of all the atoms and local spin density approximation (LSDA) exchange-correlation potential were used in the calculations. A 150 Ry energy cutoff and $1 \times 1 \times 100$ k-point grids in the Brillouin zone were adopted in order to balance the calculation accuracy and efficiency. The lattice geometric structures were fully relaxed until the convergence criteria of energy and force of 1×10^{-5} eV and 0.02 eV/Å were fulfilled, respectively. The spin-dependent currents I_σ through the device were calculated by the Landauer-Büttiker formula [38]:

$$I_\sigma(V) = \frac{e}{h}\int_{\mu_R}^{\mu_L} T_\sigma(E, V)[f_L(E-\mu_L) - f_R(E-\mu_R)]dE \tag{1}$$

where σ represents the spin-up/down (↑/↓) state, and $\mu_{R/L} = E_F \pm eV/2$ denotes the electrochemical potential of the right/left electrode. $f_{L/R}(E)$ is the Fermi-Dirac distribution function of the left/right electrode. Since the Fermi energy E_F is set to be zero, the region of the energy integral window $[\mu_L, \mu_R]$ can be written as $[-eV/2, eV/2]$. For each spin state, the electron transmission coefficient $T_\sigma(E, V)$ can be expressed as

$$T_\sigma(E, V) = Tr[\Gamma_L G^R \Gamma_R G^A]_\sigma \tag{2}$$

where $G^{R(A)}$ represents the advanced and retarded Green's function of the scattering region.

We first calculated the band structures of the two heterostructures and the results can be found in Fig. 1(c)–(d). Interestingly, band structures characteristic of half-metallic properties is observed in both heterostructures. For instance, in the case of C-B interface [Fig. 1(c)], the spin degeneracy is lifted near the Fermi level and the spin-up channel is metallic while the spin-down channel is semiconducting (with a band gap of about 0.25 eV). However, it is just the opposite in the case of C-N interface [Fig. 1(d)], i.e., semiconducting and metallic properties are obtained for the spin-up and spin-down channels, respectively. As a result, both heterostructures have intrinsic half-metallic electronic properties and the devices are very promising in spintronic applications [34]. Moreover, we also calculated the band structures of pristine ZGNR and ZBNNR. It is clear to see in Fig. 1 (e) and (f) that both bands are spin unpolarized. Furthermore, the pristine ZGNR has no band gap, and its valence and conduction bands cross at Fermi energy level. While the pristine ZBNNR has a wide band gap of about 4.5 eV.

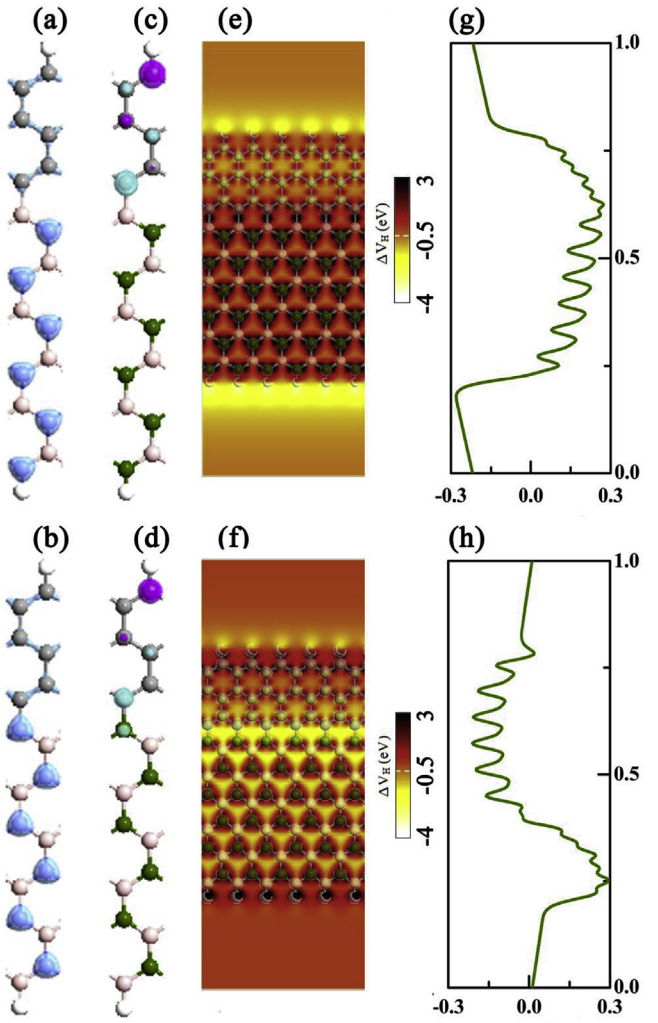

Fig. 2. (Color online) (a) and (b) Distribution of the charge density (ρ↑ + ρ↓) in the M1 and M2 devices, respectively. (c) and (d) Distribution of the spin polarization density (ρ↑-ρ↓) in the M1 and M2 devices, respectively. (e), (g) and (f), (h) Distribution of average electrostatic difference potential in the M1 and M2 devices, respectively. (For interpretation of the references to color in this figure legend, the reader is referred to the Web version of this article.)

To understand the origin of the half-metallicity the distributions of charge density (ρ↑ + ρ↓) and spin polarization density (SPD) (ρ↑-ρ↓) in the devices were calculated and the results are displayed in Fig. 2. Since the *h*-BN has a graphene-like hexagonal lattice, B (pink) and N (blue) atoms respectively occupy the A and B sublattices. Due to the stronger electronegativity, the nitrogen sites are energetically more favorable for electrons such that the charge density (ρ↑ + ρ↓) majorly distributes on the N sites (shown in Fig. 2(a) and (b)). However, little SPD distribution can be observed in the *h*-BN segment of the heterostructure, as shown in Fig. 2(c) and (d). This is because the narrow graphene segment has two edge states that are oppositely spin polarized, as revealed previously in